

## Scanning tunnelling microscopy of MgO ultrathin films on Ag(001)

S. Valeri,<sup>1,2</sup> S. Altieri,<sup>1</sup> U. del Pennino,<sup>1,2</sup> A. di Bona,<sup>1</sup> P. Luches,<sup>1,2</sup> and A. Rota<sup>1,2</sup>

<sup>1</sup>*Istituto Nazionale per la Fisica della Materia, Unità Ricerca di Modena, via Campi 213/a, 41100 Modena, Italia*

<sup>2</sup>*Università di Modena e Reggio Emilia, Dipartimento di Fisica, via Campi 213/a, 41100 Modena, Italia*

(Received 23 January 2002; published 29 May 2002)

The morphology of ultrathin epitaxial MgO layers reactively grown on Ag(001) was investigated by using scanning tunnelling microscopy. In the initial deposition stage Ag atoms are partially removed from the substrate and form extended monoatomic islands leaving vacancy islands in the substrate itself. On individual substrate terraces Ag is thereafter found at three atomic levels. For submonolayer deposition MgO condensates in form of small islands of monoatomic height, located on the original substrate, on the protruding Ag islands and on the vacancy islands as well. The largest Ag(001) fractional coverage by monoatomic MgO islands is 70%. A limited amount of MgO bilayers or trilayers has also been detected (about 1% fractional coverage). At the nominal deposition of 1 ML flat, squared and connected MgO domains of about 10 nm in width form, with edges along the [110] directions. The actual substrate fractional coverage is about 85% and the occurrence of bilayers and multilayers becomes significant (about 30 and 5% fractional coverage, respectively), resulting in the formation of three-dimensional pyramidal MgO islands.

DOI: 10.1103/PhysRevB.65.245410

PACS number(s): 68.55.-a, 68.35.Ct, 68.37.Ef, 77.55.+f

### INTRODUCTION

The MgO/Ag(001) system is an attractive model system of simple metal oxides thin films on metal substrates. These films have attracted growing interest in recent years, due to their importance for basic understanding of the metal-oxide interface and for a number of technological applications related to the demand of new generation of electronic devices, of efficient protective coatings and of stable metal catalyst supports.<sup>1,2</sup> The MgO/Ag(001) system has a square-to-square overlayer-substrate relationship with a small lattice misfit (2.9%), therefore a reduced number of dislocations is expected, mainly shifted from the hard oxide layer to the comparatively soft metal substrate. Both chemical and charge transfer contributions to bonding are believed to be negligible.<sup>3</sup> Reactions kinetics of oxygen with the Ag(001) surface is very slow,<sup>4</sup> thus the substrate oxidation is reduced in this system with respect to more reactive substrates. Finally, experimental investigation by electron spectroscopies is not inhibited by charging effects typical of insulating surfaces. Different preparation procedures of MgO(001) films on Ag(001) were comparatively investigated, including sputter deposition from bulk MgO target, oxidation of predeposited Mg film and deposition of Mg in a controlled oxygen atmosphere. It has been demonstrated that deposition of Mg in an O<sub>2</sub> atmosphere leads to much better oxide films than oxidation of predeposited Mg layers.<sup>5,6</sup> It has been also demonstrated that sputter deposition enhances the tendency of MgO to agglomerate initially in multilayered islands on Ag(001) substrate.<sup>7</sup> Structural studies performed on this system include morphology, defectivity, strain and interfacial atomic arrangement.<sup>5-13</sup>

In this paper, we present a scanning tunnelling microscopy (STM) study of ultrathin MgO films on Ag(001) prepared by reactive Mg deposition. The feasibility of using STM to study the surface structure of thin metal oxide layers was already explored for MgO films on Mo(001) and for Al<sub>2</sub>O<sub>3</sub> films on NiAl(110).<sup>15</sup> Measurements over a range of

film thickness and tunnelling parameters were performed. Stable tunnelling and imaging were obtained for MgO films up to 25 Å thick.<sup>14</sup> STM has been used to investigate the growth, structure, and electrical characteristics of the MgO/Fe(001) system.<sup>16</sup> Morphology evolution from submonolayer to monolayer(s) coverage has been studied by STM for NiO and CoO films on Ag(001),<sup>17,18</sup> and for NiO films on Cu(111).<sup>19</sup> On these systems a very complex interfacial morphology has been reported for the initial deposition stage, including oxide-induced disruption of the substrate. Recently, the electronic structure and the morphology of ultrathin MgO films on Ag(001) have been determined by scanning tunnelling spectroscopy (STS) and STM measurements, and by *ab initio* calculation of the local density of states using density functional theory.<sup>13</sup> The aim of the present work is to quantitatively investigate the very early stage of the MgO formation on Ag(001), with emphasis on the evolution of the morphology as a function of the coverage in the 0.25 to 1.25 ML deposition range.

### SUBSTRATE PREPARATION AND MgO GROWTH

The Ag(001) substrate used in the present experiment were cleaned by repeated cycles of ion bombardment and annealing, until (i) low-energy electron diffraction (LEED) showed a satisfactory pattern, with sharp spots [full width at half maximum (FWHM)  $\leq 0.14 \text{ \AA}^{-1}$ ] and high ( $\geq 8$ ) spot-to-background intensity ratio, (ii) XPS analysis revealed less than 0.5% of impurities at the surface, and (iii) STM images showed atomically stepped surfaces of high degree of perfection, with no adatom or vacancy islands. MgO layers were deposited at 470 K by Mg evaporation from a calibrated Knudsen cell, in a O<sub>2</sub> background atmosphere. The rate of oxide formation was about 1 ML min<sup>-1</sup>, as evaluated by the Mg deposition rate and the relative Mg density in metallic Mg and in MgO. The product of the deposition time and the MgO deposition rate will be referred to as nominal deposition and expressed in units of layer equivalents.

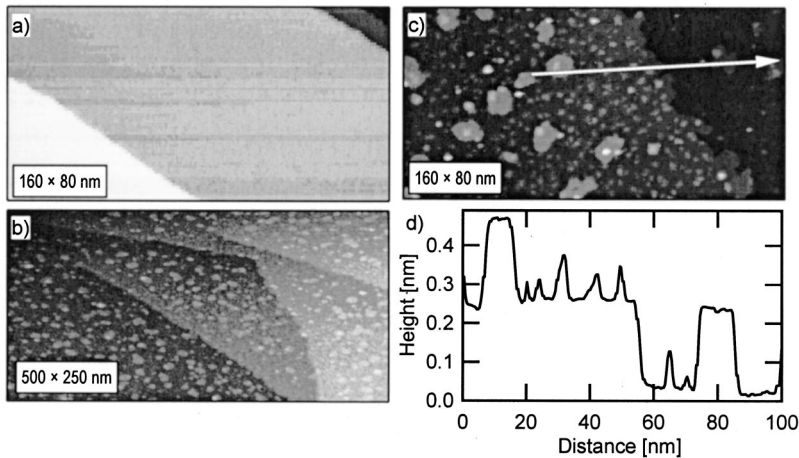


FIG. 1. (a)  $80 \times 160 \text{ nm}^2$  STM image of the Ag(001) substrate, showing large terraces separated by monoatomic or biatomic steps (0.3 V, 0.3 nA). (b)  $250 \times 400 \text{ nm}^2$  STM image of 0.25 ML MgO nominal deposition (1 V, 0.3 nA). (c)  $80 \times 160 \text{ nm}^2$  STM image of 0.25 ML MgO nominal deposition (1 V, 0.3 nA). (d) Plot of topographical height vs position along the line in panel (c).

The stoichiometry, the crystalline order and the growth mode of the MgO film were monitored *in situ* using primary beam diffraction modulated electron emission (PDMEE), AES/XPS intensity evolution, and LEED pattern analysis.<sup>8</sup> It was found that MgO grows pseudomorphically on Ag(001) with an epitaxial relationship  $\text{MgO}(001)[100]//\text{Ag}(001) \times [100]$ . For a nominal MgO deposition as low as 3 ML, a 3% expansion of the vertical lattice constant occurs in the overlayer, to accommodate the mismatch with the substrate. For larger coverage a lattice relaxation sets in, resulting in a progressive removal of the MgO tetragonal distortion.

Surface topography of MgO films was studied using STM. STM data were acquired at room temperature in the form of constant current topographies (CCT's) for two different values of the sample-bias voltage, namely, 1 and 3 V, and 0.3 nA.

### STM RESULTS AND DISCUSSION

The Ag(001) substrate shows large terraces separated by monoatomic steps, with mean separation of more than 100 nm (that correspond to a surface miscut of  $<0.1^\circ$ ) [Fig. 1(a)]. Figure 1(b) is an overview image of the Ag(001) surface after the nominal deposition of 0.25 ML of MgO, showing that the MgO-induced features are quite uniformly distributed over very large substrate areas. Figure 1(c) is an  $80 \times 160 \text{ nm}^2$  STM image of the same surface. The CCT overcompasses two substrate terraces. Several gray tone levels can be easily recognized on the individual terraces, suggesting that a quite complex morphology sets in on the Ag(001) surface upon MgO deposition. A limited number of flat extended islands are detected on both terraces, and a large number of small, less-defined islands are detected on the substrate surface and on top of the large islands as well. The shape of both large and small islands is random, and the substrate coverage is quite uniform, with the relevant exception of a reduced density of large islands in the proximity of the substrate step edges. At variance with the clean substrate, the Ag step edge no longer follows a straight line but is very rough. The plot of the “topographical” height vs position along a straight line [Fig. 1(d)] shows a distribution of values. In particular the height of the substrate step edge and of the extended islands is  $0.20 \pm 0.02 \text{ nm}$ , while the height of

the smaller islands is in the 0.06 to 0.12 nm range. Assignment of the features in STM images directly to the topography of the MgO on Ag substrate is not straightforward, because (i) the atomic step height along the surface normal direction is very similar for the overlayer and the substrate and (ii) STM imaging of ultrathin insulating films requires a proper choice of sample-bias voltage.

To obtain a topographic image of the MgO surface one needs in fact to establish tunnelling from the occupied states of the STM tip into the conduction band of MgO. For ultrathin MgO layers the band gap is expected to be lower than the bulk value, and has been reported to increase from 5 to 7.6 eV as the MgO film thickness varies from 2 to 6 ML.<sup>16</sup> Assuming that the Fermi level of MgO lies at about midgap, one would expect the optimum bias voltage to be close to +3 eV. A bias of 3 V has been already reported to be sufficient to image MgO films on Mo(001).<sup>14</sup> At a lower bias voltage the electrons tunnel directly from the tip to the conducting substrate and the oxide layer only modulates the potential barrier as a function of position. A contrast due to the oxide may still be observed because the overlayer can effectively lower the barrier. However, since the tunnel probability is a much stronger function of barrier width than of barrier height, the observed step heights would be significantly smaller under the low bias conditions. On the MgO/Ag(001) system, we observed changes in the CCT images by varying the bias voltage between 0.3 and 6.0 V, mainly as far as the height of the different features is concerned. Changes roughly saturate between 2 and 3 V, and for larger voltages the images significantly deteriorate. Therefore identification of the variety of structures observed in the CCT image of the MgO exposed Ag surfaces has been done by varying the sample-bias voltage. In fact we expect that moving the bias value from 1 to 3 V the measured height of MgO steps will change, while the Ag step height should be essentially independent of the bias.

In Fig. 2 the STM image of 0.25 ML MgO nominal deposition is shown, corresponding to the right bottom corner of Fig. 1(c), measured with a bias of 1 and 3 V [panels (a) and (b), respectively]. The topographic images look quite similar. Plots of the topographical height vs position along the same straight line [panels (a') and (b'), respectively] show that the height of the larger islands is unaffected by the bias

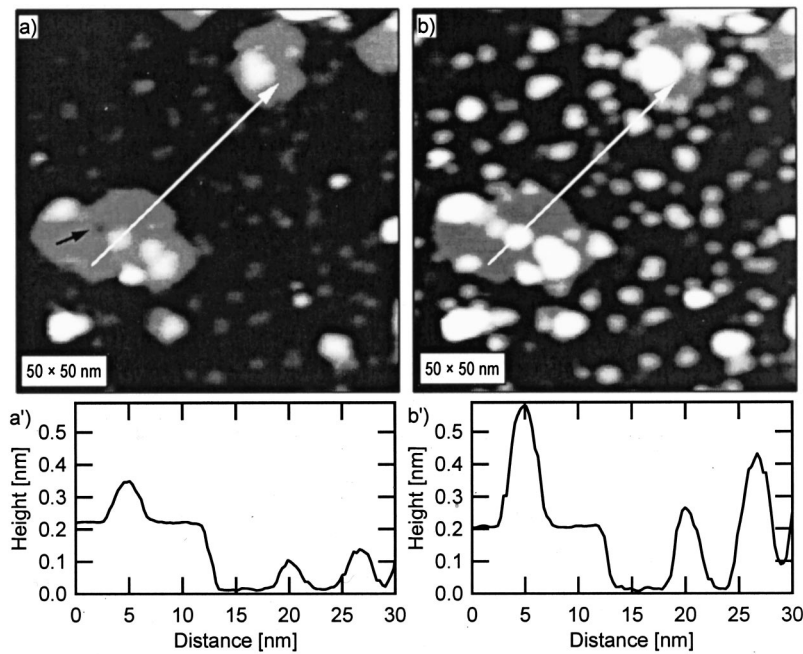


FIG. 2.  $50 \times 50 \text{ nm}^2$  STM image of 0.25 ML MgO nominal deposition: (a) 1 V and 0.3 nA, (b) 3 V and 0.3 nA. Plots of topographical height vs position along the lines are shown in (a') and (b'), respectively.

change. Larger islands are therefore identified as Ag islands protruding from the original Ag surface. The step height of the smaller islands is on the contrary very sensitive to changes in the bias voltage. In addition the values of  $0.20 \pm 0.03$  and  $0.40 \pm 0.04$  nm measured at 3 V bias are fully consistent with a single or double interplanar distance between the MgO (001) planes. Therefore we unambiguously identify these small islands as MgO islands forming mono or biatomic atomic reliefs on the Ag substrate or on the Ag large islands.

The formation of Ag islands on the substrate is expected to leave vacancy islands in the substrate itself. However, part of these vacancy islands is possibly filled by the MgO deposit, therefore only a close inspection of CCT images enables the identification of such a features. In Fig. 3(a) the same STM image of Fig. 2(a) is shown. The contrast has

been enhanced to emphasize changes in the lower range of the topographical height scale. A number of vacancy islands can be observed on the Ag substrate, some of those clearly containing small MgO aggregates [Figs. 3(b), 3(c)]. In turn, formation of vacancy islands is expected to occur also on the protruding Ag islands. Actually Fig. 2(a) shows the occurrence of a MgO-filled vacancy island on the largest Ag island. However, there is no evidence of the formation of further Ag layers on top of the Ag islands, indicating that in this case the removed atoms mainly diffuse on the island surface and condensate at the island perimeter. Roughening of the substrate step edges [clearly observed in Fig. 1(c)] occurs by both the attachment of Ag islands condensed on the lower terrace and the attachment of vacancy islands nucleated on the upper terrace. The morphology of the step edges suggests that the first mechanism is the most relevant. The very com-

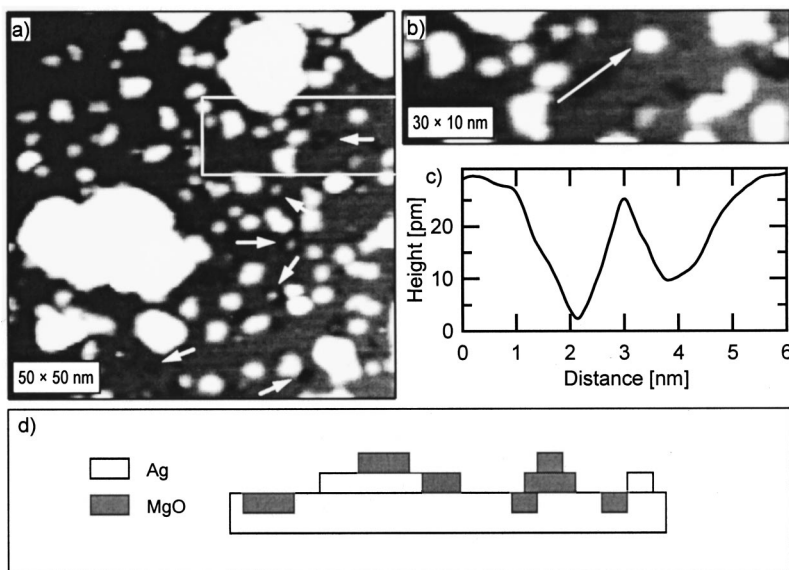


FIG. 3. (a) The same as Fig. 2(a). The contrast has been enhanced to emphasize changes in the lower range of the topographical height scale. (b)  $10 \times 30 \text{ nm}^2$  STM image of 0.25 ML MgO nominal deposition (1 V, 0.3 nA): a number of vacancy islands can be observed on the Ag substrate, some of those clearly containing small MgO aggregates (arrows). (c) Plot of topographical height vs position along the line in panel (b). (d) Sketch of the morphology of the MgO/Ag(001) interface.

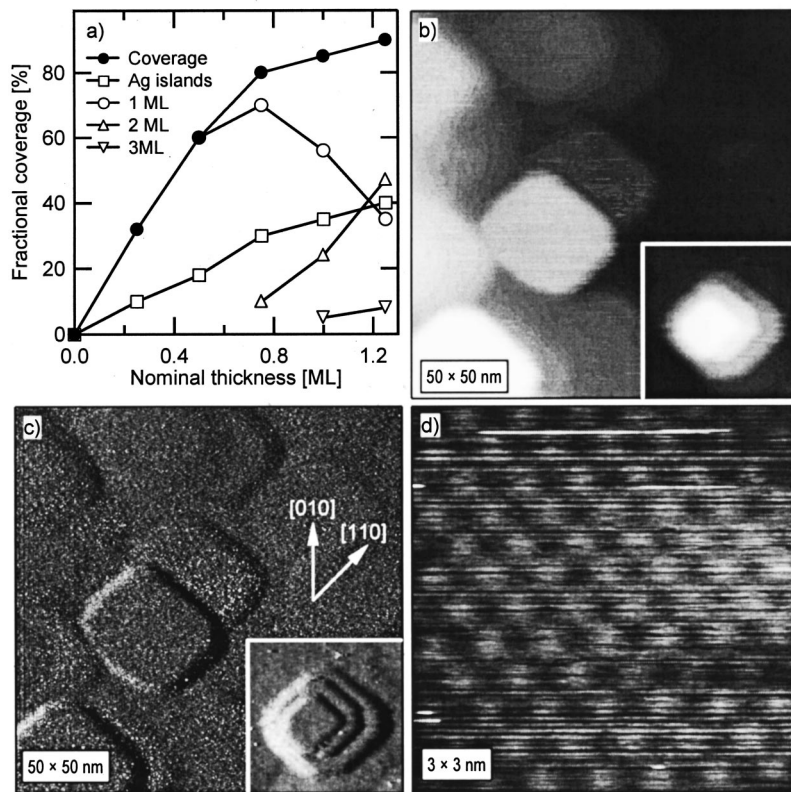


FIG. 4. (a) Fraction of Ag substrate covered by Ag islands, and fraction of Ag substrate covered by MgO layer, as a function of the nominal MgO deposition; for nominal deposition of 0.75 ML or larger, the separate contributions of single and multiple MgO layers to the coverage are also shown. (b) STM image of 1 ML MgO nominal deposition (1 V, 0.3 nA). The inset shows a multilayer MgO island. (c) Current image of the same region of panel (b). (d) Atomically resolved STM image of the top layer of the pyramid of panel (b) (1 V, 0.3 nA).

plex morphology of the MgO/Ag(001) interface at submonolayer deposition is summarized in Fig. 3(d). We notice that a qualitatively similar interfacial morphology has been reported for NiO on Cu(111) (Ref. 19) and for NiO and CoO on Ag(001).<sup>18</sup> On Ref. 18, the temperature effect on the oxide/Ag interface morphology has been mainly investigated. We focused, on the contrary, on a quantitative study of the MgO/Ag(001) interface as a function of the amount of deposited oxide.

As the nominal thickness of the deposited MgO increases, the interfacial morphology also evolves. This evolution is quantified in Fig. 4(a). The fraction of the Ag substrate covered by Ag islands increases from 10% at 0.25 ML to about 35% at 1 ML nominal deposition. In parallel, the fraction of the Ag surface (including the original substrate, the protruding islands and the vacancy islands) covered by the MgO layer also increases, from about 30% to about 85%. The largest Ag(001) fractional coverage by monoatomic MgO islands is about 70% and is reached at 0.75 ML nominal deposition. At 1 ML deposition the CCT's exhibit flat, squared and connected MgO domains, with edges along the [110] symmetry directions [Figs. 4(b), 4(c)]. The presence of a limited amount of bilayers or trilayers of MgO has been detected at 0.75 ML MgO deposition, and becomes significant at 1 ML deposition [Fig. 4(a)], resulting in the formation of 3D pyramidal islands [inset of Figs. 4(b), 4(c)]. Again, edges of the pyramids are oriented along the [110] directions. A square shape was observed for four layers thick MgO islands on Fe(001).<sup>16</sup> Three layers thick MgO islands with the edges oriented along the [110] directions were observed for MgO films grown on Mo(001) at substrate temperatures in excess

of 1100 K.<sup>14</sup> Oxide islands with edges along the [110] symmetry directions have been also observed for submonolayer deposition of NiO on Ag(001), in contrast to the CoO case where the orientation of the island edges was along the [100] direction.<sup>18</sup> [100] oriented oxide islands can be observed in the STM images of thin MgO films on Ag(001).<sup>13</sup>

Atomic resolution on top of the pyramid appearing in the inset of Fig. 4(c) is shown in Fig. 4(d). The observed surface lattice constant has twice the value of the surface lattice constant of MgO, indicating that only one type of ion is imaged. The lattice is free of local defects and appears almost perfectly arranged.

Layer-by-layer growth is thermodynamically favored when the surface energy of the overlayer is significantly low in comparison to that of the substrate. This is the case, e.g., for the MgO/Fe(001) system, that in fact has been reported to grow in a nearly perfect layer-by-layer mode.<sup>16</sup> The STM data discussed in the present paper show that the bidimensional growth is favored also for the MgO/Ag(001) case, in spite of the very similar surface energies of MgO (1.16 J/m<sup>2</sup>) (Ref. 20) and Ag (1.30 J/m<sup>2</sup>).<sup>21</sup> In fact in the submonolayer deposition range a sharp MgO(100)/Ag(001) interface is obtained via formation of monoatomic MgO islands covering most of the Ag(001) surface. Nominal deposition up to 0.5 ML yield nucleation of perfectly two-dimensional monoatomic MgO terraces.

## CONCLUSIONS

We reported on a detailed quantitative investigation of the evolution of the MgO/Ag(001) interface morphology vs the

oxide thickness in the 0.25–1.25 ML range. The STM results indicate that the reactive deposition of MgO on Ag(001) surface leads to a very complex morphology. Substrate disruption occurs, with formation of vacancy islands and protruding Ag islands. At submonolayer deposition, small MgO islands form on the Ag substrate, and on vacancy and protruding islands as well. The MgO islands are mainly monoatomic in height, but a limited amount of bilayers or trilayers is also present. For increasing deposition both the substrate fractional coverage and the fraction of multilayer islands increase. At 1 ML nominal deposition the substrate fractional coverage is about 85%, with formation of flat, squared MgO domains of about 10 nm in width. A relevant number of 3D pyramidal MgO islands with edges along the [110] symmetry directions is present. The morphology of the 1 ML film is

consistent with the results reported in Ref. 13, except for the different orientation of the island edges. The dependence of the topographic height on the sample bias voltage has been found to be a useful criterion for the identification of Ag and MgO features in the STM images.

#### ACKNOWLEDGMENTS

The authors are indebted to G. Pacchioni and C. Pisani for the useful discussions. Financial support by Istituto Nazionale per la Fisica della Materia (Advanced Research Project ISADORA) and by Ministero della Ricerca Scientifica e Tecnologica-Programmi di Ricerca di Rilevante Interesse Nazionale 99, is gratefully acknowledged.

- 
- <sup>1</sup>S. C. Street and D. W. Goodman, in *Growth and Properties of Ultrathin Epitaxial Layers, The Chemical Physics of Solid Surfaces*, edited by D. A. King and D. P. Woodruff (Elsevier, New York, 1997), Chap. 10.
- <sup>2</sup>S. A. Chambers, *Surf. Sci. Rep.* **39**, 105 (2000).
- <sup>3</sup>C. Li, R. Wu, A. J. Freeman, and C. L. Fu, *Phys. Rev. B* **48**, 8317 (1993).
- <sup>4</sup>C. S. Ares Fang, *Surf. Sci.* **235**, L291 (1990).
- <sup>5</sup>J. Wollschläger, J. Viernow, C. Tegenkamp, D. Erdös, K. M. Schröder, and H. Pfnür, *Appl. Surf. Sci.* **142**, 129 (1999).
- <sup>6</sup>C. Tegenkamp, H. Pfnür, W. Ernst, U. Malasake, J. Wollschläger, D. Peterka, K. M. Schröder, V. Zielasek, and M. Henzler, *J. Phys.: Condens. Matter* **11**, 9943 (1999).
- <sup>7</sup>S. Valeri, S. Altieri, A. di Bona, C. Giovanardi, and T. S. Moia, *Thin Solid Films* **400**, 16 (2001).
- <sup>8</sup>S. Valeri, S. Altieri, A. di Bona, P. Luches, C. Giovanardi, T. S. Moia, and A. Rota, *Surf. Sci.* (to be published).
- <sup>9</sup>J. Wollschläger, D. Erdös, and K. M. Schröder, *Surf. Sci.* **402–404**, 272 (1998).
- <sup>10</sup>D. Peterka, C. Tegenkamp, K. M. Schröder, W. Ernst, and H. Pfnür, *Surf. Sci.* **431**, 146 (1999).
- <sup>11</sup>J. Wollschläger, D. Erdös, H. Goldbach, R. Hopken, and K. M. Schröder, *Thin Solid Films* **400**, 1 (2001).
- <sup>12</sup>M. Sgroi, C. Pisani, and M. Busso, *Thin Solid Films* **400**, 64 (2001).
- <sup>13</sup>S. Schintke, S. Messerli, M. Pivetta, F. Patthey, L. Libioulle, M. Stengel, A. De Vita, and W.-D. Schneider, *Phys. Rev. Lett.* **87**, 276801 (2001).
- <sup>14</sup>M. C. Gallagher, M. S. Fyfield, J. P. Cowin, and S. A. Joyce, *Surf. Sci.* **339**, L909 (1995).
- <sup>15</sup>Th. Bertrams, A. Brodde, and H. Neddermeyer, *J. Vac. Sci. Technol. B* **12**, 2122 (1994).
- <sup>16</sup>M. Klaua, D. Ullmann, J. Barthel, W. Wulfhekel, J. Kirschner, R. Urban, T. L. Monchesky, A. Enders, J. F. Cochran, and B. Heinrich, *Phys. Rev. B* **64**, 134411 (2001).
- <sup>17</sup>T. Bertrams and H. Neddermeyer, *J. Vac. Sci. Technol. B* **14**, 1141 (1996).
- <sup>18</sup>I. Sebastian, T. Bertrams, K. Meinel, and H. Neddermeyer, *Faraday Discuss.* **114**, 129 (1999).
- <sup>19</sup>S. Stanesco, Ch. Boeglin, A. Barbier, J.-P. Deville, J. Hommet, and R. Lazzari (unpublished).
- <sup>20</sup>P. W. Tasker and D. M. Druffy, *Surf. Sci.* **137**, 91 (1984).
- <sup>21</sup>L. Z. Mezey and J. Giber, *Jpn. J. Appl. Phys.* **21**, 1569 (1982).